Optimizing surface defects for atomic-scale electronics: Si dangling bonds

Peter Scherpelz[1,*] and Giulia Galli[1,2]

[1]*Institute for Molecular Engineering, The University of Chicago, Chicago, Illinois 60637, USA*
[2]*Materials Science Division, Argonne National Laboratory, Argonne, Illinois 60439, USA*

Surface defects created and probed with scanning tunneling microscopes are a promising platform for atomic-scale electronics and quantum information technology applications. Using first-principles calculations we demonstrate how to engineer dangling bond (DB) defects on hydrogenated Si(100) surfaces, which give rise to isolated impurity states that can be used in atomic-scale devices. In particular, we show that sample thickness and biaxial strain can serve as control parameters to design the electronic properties of DB defects. While in thick Si samples the neutral DB state is resonant with bulk valence bands, ultrathin samples (1–2 nm) lead to an isolated impurity state in the gap; similar behavior is seen for DB pairs and DB wires. Strain further isolates the DB from the valence band, with the response to strain heavily dependent on sample thickness. These findings suggest new methods for tuning the properties of defects on surfaces for electronic and quantum information applications. Finally, we present a consistent and unifying interpretation of many results presented in the literature for DB defects on hydrogenated silicon surfaces, rationalizing apparent discrepancies between different experiments and simulations.

The ability to engineer semiconducting devices at the atomic scale is key to achieving further miniaturization of electronics, and to using the quantum nature of point defects for quantum information applications. One promising atomic-scale fabrication method employs scanning tunneling microscopy (STM) to create and manipulate defects on semiconducting surfaces [1]. For example, dangling bonds (DBs) have been created and successfully manipulated on hydrogen-terminated Si(100) surfaces by desorbing individual H atoms from the substrate [2]. Ensembles of DBs on silicon surfaces are now widely used to create atomically precise systems of defects [3–15], leveraging expertise with the fabrication of silicon devices, including the ability to produce clean and regular hydrogen-terminated surfaces.

Numerous experiments have demonstrated many attractive properties and potential applications of DBs on H:Si(100). These defects interact over next-nearest-neighbor distances [3,4,6], and the charge of individual DBs can be reversibly manipulated, with given charge states persisting for hours [5]. In addition, these DBs display negative differential resistance, potentially providing a new component for atomic-scale electronic circuitry [12]. Theoretical work has suggested that pairs of DBs may be used to create a charge qubit [16]. Furthermore, DBs may be assembled into specific patterns for electronics or quantum simulations [6,14,17,18], including one-dimensional conducting or semiconducting wires [7,19,20]. They further serve as a starting configuration for atomically precise dopant placement [21–25]. Hence tuning and manipulating the properties of DBs, e.g., charge states, may lead to a promising strategy to build a flexible atomic-scale platform of defects for electronic and quantum information technology applications.

In this work, using the results of first-principles calculations we propose ways to realize DB defect states on H:Si(100) with energies within the electronic gap of bulk Si; in particular, we show how to tune sample thickness and strain to obtain

desired energy and charge states. While doing so, we also address existing controversies present in the literature on the properties of DB states on Si surfaces. We present a consistent interpretation of previous results, and use advanced methods to ensure our findings are robust. We first show how the thickness of the Si sample can be manipulated to alter the electronic properties of the neutral Si DB state, and we demonstrate that a stable positively charged DB state is accessible only in thin (1.2 nm) Si samples. We also present similar effects for multiple DB systems. We then turn our attention to the effect of biaxial strain, showing that the electronic response of defects to strain depends significantly on the slab thickness. We propose that by combining thickness and strain, one may engineer the properties of neutral DB defects for use in atomic-scale electronics.

Methods. We carried out density functional theory (DFT) [26,27] calculations with plane-wave basis sets and norm-conserving pseudopotentials [28,29] using the QUANTUM ESPRESSO package [30,31]. We modeled Si DBs on an H-terminated Si(100) slab periodically repeated in two directions and having a finite number of layers in the third, with vacuum separating periodic images. All neutral DB calculations were spin polarized. Atomic geometries were optimized until forces on the atoms were less than 0.013 eV/Å.

We used the gradient-corrected exchange-correlation functional developed by Perdew, Burke, and Ernzerhof (PBE) [32], as well as hybrid functionals [33]. In particular, we adopted a dielectric-dependent hybrid with the fraction of exact exchange $\alpha = 0.085 \approx 1/\epsilon_\infty^{Si}$, shown to reproduce accurately the electronic properties of bulk Si [34]. We also used the Heyd-Scuseria-Ernzerhof (HSE) functional [35,36] to compare with previous work. In addition, for selected configurations we performed many-body perturbation theory (MBPT) calculations [37–39] at the G_0W_0 level using the WEST software package [40–42]. Within G_0W_0 the exchange-correlation energy entering DFT is replaced by an electronic self-energy calculated using the screened Coulomb interaction and the Green's function. WEST uses spectral decomposition
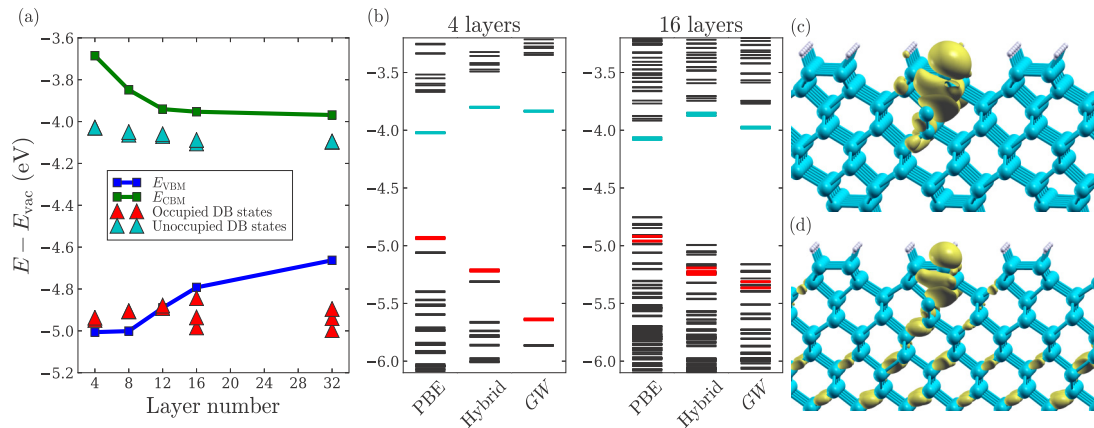
---
*pscherpelz@uchicago.edu

FIG. 1. Electronic properties of neutrally charged dangling bonds on an H-terminated Si(100) slab. (a) Variation of the VBM, CBM, and DB energy levels with layer number included in a model Si slab, as obtained using DFT calculations at the PBE level. We estimate that for slab thicknesses of 8 nm or greater, the DB position is about 0.3 eV below the VBM. (b) Energy levels at the Γ point of the slab Brillouin zone, as obtained with DFT using gradient-corrected (PBE) and dielectric-dependent hybrid functionals, and many-body perturbation theory calculations (GW). Results for 4- and 16-layer slabs are displayed. As in (a), red (cyan) designates energy levels of occupied (unoccupied) DB states. (c) Isosurface of the wave-function amplitude for an isolated DB state in an H-terminated eight-layer Si slab. (d) Isosurface of the wave-function amplitude for a DB state hybridized with a bulk state in an H-terminated 16-layer Si slab (see SM for details).

techniques [40,43–46] and methods based on density functional perturbation theory [47] to optimize calculations for large systems [40].

Details of geometries, calculation parameters, convergence tests, and identification of DB states, can be found in the Supplemental Material (SM) [48].

Results. Multiple computational results have been reported in the literature for the singly occupied, neutral DB (DB^0) state, relative to the valence-band maximum (VBM) of Si: -0.3 eV [49], 0.013 eV [6], 0.2 eV [50], 0.35 eV [16,51], 0.36 eV [7], and 0.42 eV [52] (other calculations [5,11,53] only addressed doped systems and/or charged DBs) [54]. These results differ quantitatively and qualitatively: indeed, a defect state located in energy above the VBM is expected to be well isolated electronically, whereas one below may instead hybridize with other electronic states in the material and hence may not be amenable to manipulation.

In order to rationalize the various literature values for the DB^0, we calculated its electronic properties for many model slabs, differing by the number of layers and supercell lattice constant. We found that the choice of lattice constants in the plane perpendicular to the surface primarily influenced the degree of dispersion of the DB state (see SM for details). We observed instead a much more pronounced dependence of the nature of the DB state on the thickness of the slab, as shown in Fig. 1(a). Its energy relative to the vacuum energy of the supercell model is roughly constant. However, the positions of the VBM and conduction-band minimum (CBM) vary significantly with the number of layers in the slab. In general, quantum confinement leads to a larger band gap whose convergence toward the bulk value is very slow as a function of the slab layer number [55,56]. A similar dependence on thickness was recently found for a bare Si(100)-$p(2\times2)$ surface [57].

Figure 1(a) shows that for a slab eight layers thick ($\approx$ 1.2 nm) the DB energy is 0.09 eV above the VBM energy,

while for a 16-layer slab ($\approx$ 2.3 nm) its energy is 0.05–0.19 eV below the VBM energy. The DB^0 state is well isolated for eight or fewer layer slabs, while it is mixed with bulk Si states for 16 or more layers, as shown in Figs 1(c) and 1(d). To verify these findings are robust with respect to the level of theory used, we carried out additional calculations using dielectric-dependent hybrid functionals and MBPT. Figure 1(b) shows that the position of the occupied DB state relative to the VBM is nearly the same at all levels of theory. Hybrid and GW calculations significantly correct the band-gap energy found at the PBE level, but leave the DB state positions relative to the VBM and CBM unchanged.

Hence we conclude that for Si samples 1.2 nm or thinner, the neutral singly occupied DB state falls within the bulk gap, while for samples 2.3 nm or thicker, it is hybridized with bulk states and resides below the VBM. We expect the DB^0 state to have a much shorter coherence time for thickness > 2.3 nm, impacting its behavior in quantum information applications. However, in other applications, its hybridization with bulk states of thick slabs may be beneficial by facilitating long-range interactions between point defects.

We note that these DB properties are different from those of Si DBs at a Si/SiO$_2$ interface, for which the energy of the neutral defect is found by electron paramagnetic resonance to reside in the gap of bulk Si [58]. This difference is presumably due to the significantly different environment surrounding DBs in the two systems [52]. We also stress that the behavior above is not due to a change in the net magnetization density (which is not significant as a function of layer thickness), but rather is due to changes in the energy level of the singly occupied DB, which is an isolated defect state for thin slabs but a resonant defect state for thick slabs.

While understanding the properties of the neutral DB is important for potential quantum information applications, charge transition energy levels (CTLs) are the quantities of interest for scanning tunneling spectroscopy observations
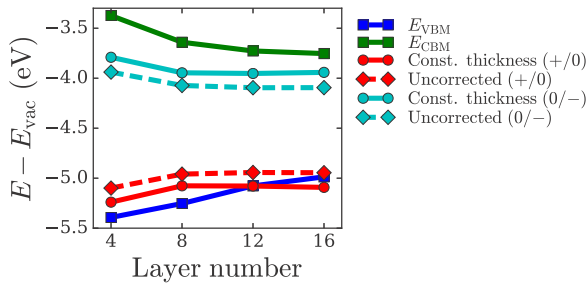
FIG. 2. Calculated adiabatic charge transition levels of a DB on an H-terminated Si(100) surface, as a function of the sample thickness, using the dielectric-dependent hybrid functional. E_{VBM} and E_{CBM} indicate the energies of the valence-band minimum and the conduction-band maximum, respectively. Uncorrected results omit the finite-size scaling corrections obtained with the method of Ref. [53].

[5,7–12], and applications for electronics [5,12] or charge qubits [16]. We obtained CTLs by computing total energies of different charge states in their respective optimized geometries (thus calculating adiabatic transitions), taking into account corrections for the Coulomb interaction of periodic images, and alignment of the electrostatic potential between configurations [59]. For surfaces, correction methods used in bulk systems are not applicable due to the large variation in dielectric constant between the bulk and vacuum. We followed the prescription suggested in Ref. [53]. Briefly, a sawtooth electric field is used to compute the z-dependent dielectric constant, from which a periodic electrostatic model of the charged defect is constructed. The electrostatic energy is then calculated using finite-size scaling by extrapolating the energy of the model computed for cells of increasing sizes. As we were interested specifically in the properties of thin Si slabs, we kept the slab height constant during extrapolation.

Calculations at the PBE level of theory were performed to check for convergence, and consistent results were found, within ±0.1 eV, when varying vacuum length of the supercell by a factor of 2 and horizontal supercell area by a factor of 2.7. Figure 2 shows our results using the dielectric-dependent hybrid functional. Qualitatively, the PBE results are similar to those in Fig. 2, with a 0.2 eV decrease in the (+/0) CTL relative to the VBM (see SM).

Figure 2 shows that for thick samples (> 2.3 nm), only the (0/−) CTL falls within the bulk Si band gap. This result is consistent with the experimental observation showing long lifetimes of both the DB^0 and DB^- charge states, when the DB is appropriately charged by an STM tip which is then removed [5]. No long-lived DB^+ state was detected experimentally, even though a p-type Si sample was used [5]. Interestingly, Fig. 2 also shows that very thin samples may exhibit long-lived DB^+ states without requiring any other perturbations, making all three charge states easily accessible. Such a system may provide a flexible platform for quantum information technology applications.

Arrangements of multiple DBs lead to additional possibilities for atomic-scale electronics. We considered two prototypical multiple-DB systems, and we found that they exhibit the same properties as a single DB, as a function of
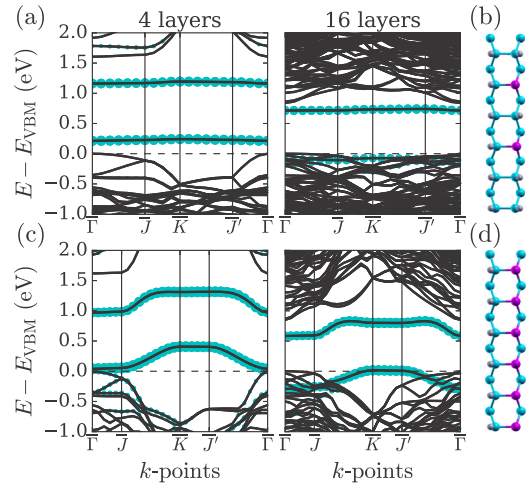

FIG. 3. Electronic properties of multiple-DB systems. (a) Band structure of a neutral DB pair. (b) Model of the DB pair system. Si DBs are highlighted. (c) Band structure of the antiferromagnetic DB wire. Cyan circles in (a) and (c) show the overlap of states with the Si atoms containing the DBs. (d) Model of the DB wire. Si DBs are highlighted. The neutral, singly occupied DBs have alternating spin-up and spin-down configurations.

thickness. Figure 3(a) shows the band structure of a neutral DB pair [4,6,16]. Its geometry [Fig. 3(b)] is an example of that proposed for charge qubits [4,16]. For a four-layer slab all DB states are well separated, while for a 16-layer slab the occupied DB states become resonant with the valence band. The presence of this resonance may lead to stronger interactions between bulk and DB states; the overall larger gap for a four-layer system should also improve addressability of the DB pair using midinfrared lasers [60].

Figure 3(c) shows the band structure of the antiferromagnetic DB wire in Fig. 3(d) [7,19,20,61–65]. For a neutral DB wire on a four-layer slab, both the occupied and unoccupied one-dimensional (1D) bands lie within the gap, and thus the wire may conduct either electron or hole states under suitable bias. In contrast, for a 16-layer slab, only the unoccupied 1D band lies within the gap, while the occupied 1D band is resonant with the bulk Si states. Thus, for 16 layers, hole conduction would be expected to occur through both bulk and wire states when a suitable bias is applied, removing the 1D nature of the conductivity.

A recent theoretical study raised the intriguing possibility of using strain to isolate surface states of a bare Si(100) surface, showing that the VBM is lowered in energy when biaxial tensile strain is applied in the horizontal directions [66]. However, this result is not consistent with those of theoretical and experimental investigations of bulk Si under biaxial tensile strain, showing that the VBM energy increases and the bulk band gap decreases [67,68]. Our results indicate that for standard (thick) silicon surfaces, strain will not isolate surface states, in contrast to the conclusions of Ref. [66]. Instead, only for thin Si slabs can strain be used to isolate surface states, a result of the remarkably different response to strain for thin slabs compared to bulk systems. Figure 4(a) shows this difference in response: the VBM position as a function of strain shows a qualitatively different trend for
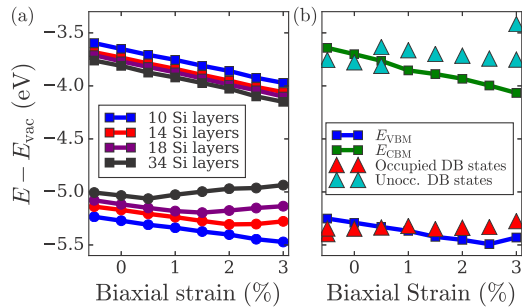
FIG. 4. Variation of electronic properties as a function of biaxial strain applied to the Si slab. (a) Variation of the VBM (circles) and CBM (squares) positions vs strain. For all values of strain, the band gap for 34-layer slabs is within 0.1 eV of the bulk band gap. (b) Variation of VBM and CBM positions, and the energies of DB states, for a 10-layer system.

thick ($\gtrsim 4$ nm) slabs, where it increases with strain, and thin (10-layer, 1.5 nm) slabs, where it decreases with strain to a thickness-dependent minimum. As a result, for thick slabs the fundamental gap remains close to that of the bulk, but for thin slabs tensile strain leads to an increase of the gap relative to that of bulk Si. An unstrained 10-layer slab has a fundamental gap 0.4 eV larger than that of bulk Si. In contrast, under 3% biaxial tensile strain its fundamental gap is 0.8 eV larger than that of the bulk.

Thus, while in thick slabs biaxial tensile strain would not be expected to aid in isolating DB states, in very thin slabs, the opposite is true, as shown in Fig. 4(b). A state which is not well isolated in a 1.5 nm unstrained slab becomes isolated for strains of 1% or more. For direct comparison with Ref. [66], results in Fig. 4 used the HSE hybrid functional; calculations with PBE showed the same trend as a function of strain (see SM). Note that Ref. [66] used a 10-layer slab model, effectively reporting results applicable only to thin slabs.

In summary, we have proposed how to engineer the properties of DBs on hydrogenated Si surfaces by varying sample thickness and applied stress. We have shown that the single particle energy and wave function of DBs on H:Si(100)-(2×1) may be more readily isolated from those of bulk states in thin samples (<1.2 nm) than in bulklike slabs. Specifically, in thin samples, the neutral DB state is well above the VBM, and three charge states may be stabilized. In thick (>2.3 nm) samples, the neutral DB state is instead hybridized with bulk states, and the positively charged DB is not stable; for bulk samples the neutral DB state is about 0.3 eV below the VBM. We verified that our results are robust with respect to the level of first-principles theory used, including semilocal and hybrid functionals and many-body perturbation theory.

Dangling bond pairs and wires showed the same response to sample thickness. Notably, thin samples allow hole conduction along isolated DB wires, whereas in thick samples conduction would also occur through the bulk. Additionally, we found that in thin samples biaxial tensile strain will further isolate the DB energy from that of the VBM. However, strain is not helpful in isolating states in thick Si samples.

We emphasize the importance of carrying out accurate calculations, numerically converged and at a high level of theory, in order to determine the properties of isolated DBs. Although numerous experimental STM studies have been performed, both tip-induced band bending and nonequilibrium charging did not allow for a clear extrapolation of results to isolated DB configurations [5–12]. Furthermore, recent work has shown that nearby dopants can affect the behavior of DBs [10], which further complicates the interpretation of experimental findings. Our study of electronic properties as a function of film thickness was able to reconcile apparent discrepancies found in published results, which were reported for different numbers of layers in the slabs and sometimes interpreted as representative of bulk samples (we estimate that 60 layers are necessary for calculations to be representative of thick, bulklike samples).

A question remains on the experimental realization of the thin films proposed here as promising platforms. Si films as thin as 3 nm have been reported [69]; strained Si-on-insulator samples less than 10 nm thick have also been fabricated [70]. While the 1–2-nm slabs considered here may require new techniques, their experimental realization appears possible in the near future. Finally, we expect the results found here for DBs may be valid for several other defects when placed in thin Si slabs. This includes many defects used in quantum information applications, such as isolated phosphorous [71,72], boron [73], bismuth [74,75], or selenium [76,77] dopants, as well as patterned surface systems [6,14,17,18]. Indeed, the electronic properties of the DBs change as a function of thickness due to the change of the VBM and CBM themselves, not because of a substantial shift of the defect level. Hence the combination of strain and thickness proposed here to isolate DB defects and stabilize multiple charge states should be generalizable to other types of defects.

[1] F. A. Zwanenburg, A. S. Dzurak, A. Morello, M. Y. Simmons, L. C. L. Hollenberg, G. Klimeck, S. Rogge, S. N. Coppersmith, and M. A. Eriksson, Silicon quantum electronics, Rev. Mod. Phys. **85**, 961 (2013).

[2] J. W. Lyding, T.-C. Shen, J. S. Hubacek, J. R. Tucker, and G. C. Abeln, Nanoscale patterning and oxidation of H-passivated Si(100)-2×1 surfaces with an ultrahigh vacuum scanning tunneling microscope, Appl. Phys. Lett. **64**, 2010 (1994).

[3] M. B. Haider, J. L. Pitters, G. A. DiLabio, L. Livadaru, J. Y. Mutus, and R. A. Wolkow, Controlled Coupling and Occupation of Silicon Atomic Quantum Dots at Room Temperature, Phys. Rev. Lett. **102**, 046805 (2009).

[4] J. L. Pitters, L. Livadaru, M. B. Haider, and R. A. Wolkow, Tunnel coupled dangling bond structures on hydrogen terminated silicon surfaces, J. Chem. Phys. **134**, 064712 (2011).

[5] A. Bellec, L. Chaput, G. Dujardin, D. Riedel, L. Stauffer, and P. Sonnet, Reversible charge storage in a single silicon atom, Phys. Rev. B **88**, 241406 (2013).

[6] S. R. Schofield, P. Studer, C. F. Hirjibehedin, N. J. Curson, G. Aeppli, and D. R. Bowler, Quantum engineering at the silicon surface using dangling bonds, Nat. Commun. **4**, 1649 (2013).

[7] W. Ye, K. Min, P. Peña Martin, A. A. Rockett, N. R. Aluru, and J. W. Lyding, Scanning tunneling spectroscopy and density functional calculation of silicon dangling bonds on the Si(100)-2 × 1:H surface, Surf. Sci. **609**, 147 (2013).

[8] M. Taucer, L. Livadaru, P. G. Piva, R. Achal, H. Labidi, J. L. Pitters, and R. A. Wolkow, Single-Electron Dynamics of an Atomic Silicon Quantum Dot on the H-Si(100)-(2×1) Surface, Phys. Rev. Lett. **112**, 256801 (2014).

[9] M. Kolmer, S. Godlewski, R. Zuzak, M. Wojtaszek, C. Rauer, A. Thuaire, J.-M. Hartmann, H. Moriceau, C. Joachim, and M. Szymonski, Atomic scale fabrication of dangling bond structures on hydrogen passivated Si(001) wafers processed and nanopackaged in a clean room environment, Appl. Surf. Sci. **288**, 83 (2014).

[10] H. Labidi, M. Taucer, M. Rashidi, M. Koleini, L. Livadaru, J. Pitters, M. Cloutier, M. Salomons, and R. A. Wolkow, Scanning tunneling spectroscopy reveals a silicon dangling bond charge state transition, New J. Phys. **17**, 073023 (2015).

[11] H. Kawai, O. Neucheva, T. L. Yap, C. Joachim, and M. Saeys, Electronic characterization of a single dangling bond on n- and p-type Si(001)-(2 × 1):H, Surf. Sci. **645**, 88 (2016).

[12] M. Rashidi, M. Taucer, I. Ozfidan, E. Lloyd, M. Koleini, H. Labidi, J. L. Pitters, J. Maciejko, and R. A. Wolkow, Time-Resolved Imaging of Negative Differential Resistance on the Atomic Scale, Phys. Rev. Lett. **117**, 276805 (2016).

[13] T. Hitosugi, T. Hashizume, S. Heike, Y. Wada, S. Watanabe, T. Hasegawa, and K. Kitazawa, Scanning tunneling spectroscopy of dangling-bond wires fabricated on the Si(100)-2×1-H surface, Appl. Phys. A **66**, S695 (1998).

[14] L. Soukiassian, A. J. Mayne, M. Carbone, and G. Dujardin, Atomic wire fabrication by STM induced hydrogen desorption, Surf. Sci. **528**, 121 (2003).

[15] A. J. Mayne, D. Riedel, G. Comtet, and G. Dujardin, Atomic-scale studies of hydrogenated semiconductor surfaces, Prog. Surf. Sci. **81**, 1 (2006).

[16] L. Livadaru, P. Xue, Z. Shaterzadeh-Yazdi, G. A. DiLabio, J. Mutus, J. L. Pitters, B. C. Sanders, and R. A. Wolkow, Dangling-bond charge qubit on a silicon surface, New J. Phys. **12**, 083018 (2010).

[17] F. Ample, I. Duchemin, M. Hliwa, and C. Joachim, Single OR molecule and OR atomic circuit logic gates interconnected on a Si(100)H surface, J. Phys.: Condens. Matter **23**, 125303 (2011).

[18] M. Kepenekian, R. Robles, R. Rurali, and N. Lorente, Spin transport in dangling-bond wires on doped H-passivated Si(100), Nanotechnology **25**, 465703 (2014).

[19] T. Hitosugi, S. Heike, T. Onogi, T. Hashizume, S. Watanabe, Z.-Q. Li, K. Ohno, Y. Kawazoe, T. Hasegawa, and K. Kitazawa, Jahn-Teller Distortion in Dangling-Bond Linear Chains Fabricated on a Hydrogen-Terminated Si(100)-2 × 1 Surface, Phys. Rev. Lett. **82**, 4034 (1999).

[20] B. Naydenov and J. J. Boland, Engineering the electronic structure of surface dangling bond nanowires of different size and dimensionality, Nanotechnology **24**, 275202 (2013).

[21] S. R. Schofield, N. J. Curson, M. Y. Simmons, F. J. Rueß, T. Hallam, L. Oberbeck, and R. G. Clark, Atomically Precise Placement of Single Dopants in Si, Phys. Rev. Lett. **91**, 136104 (2003).

[22] F. J. Ruess, L. Oberbeck, M. Y. Simmons, K. E. J. Goh, A. R. Hamilton, T. Hallam, S. R. Schofield, N. J. Curson, and R. G. Clark, Toward atomic-scale device fabrication in silicon using scanning probe microscopy, Nano Lett. **4**, 1969 (2004).

[23] M. Fuechsle, J. A. Miwa, S. Mahapatra, H. Ryu, S. Lee, O. Warschkow, L. C. L. Hollenberg, G. Klimeck, and M. Y. Simmons, A single-atom transistor, Nat. Nanotechnol. **7**, 242 (2012).

[24] B. Weber, S. Mahapatra, H. Ryu, S. Lee, A. Fuhrer, T. C. G. Reusch, D. L. Thompson, W. C. T. Lee, G. Klimeck, L. C. L. Hollenberg, and M. Y. Simmons, Ohm's law survives to the atomic scale, Science **335**, 64 (2012).

[25] G. W. Morley, Towards spintronic quantum technologies with dopants in silicon, in *Electron Paramagnetic Resonance*, Vol. 24 (Royal Society of Chemistry, London, 2014), Chap. 3, p. 62.

[26] P. Hohenberg and W. Kohn, Inhomogeneous electron gas, Phys. Rev. **136**, B864 (1964).

[27] W. Kohn and L. J. Sham, Self-consistent equations including exchange and correlation effects, Phys. Rev. **140**, A1133 (1965).

[28] N. Troullier and J. L. Martins, Efficient pseudopotentials for plane-wave calculations, Phys. Rev. B **43**, 1993 (1991).

[29] D. Ceresoli, Pseudopotentials, https://sites.google.com/site/dceresoli/pseudopotentials (accessed May 20, 2016).

[30] P. Giannozzi, S. Baroni, N. Bonini, M. Calandra, R. Car, C. Cavazzoni, D. Ceresoli, G. L. Chiarotti, M. Cococcioni, I. Dabo *et al.*, QUANTUM ESPRESSO: A modular and open-source software project for quantum simulations of materials, J. Phys.: Condens. Matter **21**, 395502 (2009).

[31] QUANTUMESPRESSO, http://www.quantum-espresso.org (accessed Jan. 26, 2016).

[32] J. P. Perdew, K. Burke, and M. Ernzerhof, Generalized Gradient Approximation Made Simple, Phys. Rev. Lett. **77**, 3865 (1996).

[33] S. Kümmel and L. Kronik, Orbital-dependent density functionals: Theory and applications, Rev. Mod. Phys. **80**, 3 (2008).

[34] J. H. Skone, M. Govoni, and G. Galli, Self-consistent hybrid functional for condensed systems, Phys. Rev. B **89**, 195112 (2014).

[35] J. Heyd, G. E. Scuseria, and M. Ernzerhof, Hybrid functionals based on a screened Coulomb potential, J. Chem. Phys. **118**, 8207 (2003).

[36] J. Heyd, G. E. Scuseria, and M. Ernzerhof, Erratum: Hybrid functionals based on a screened Coulomb potential [J. Chem. Phys. **118**, 8207 (2003)], J. Chem. Phys. **124**, 219906 (2006).

[37] L. Hedin, New method for calculating the one-particle Green's function with application to the electron-gas problem, Phys. Rev. **139**, A796 (1965).

[38] M. S. Hybertsen and S. G. Louie, Electron correlation in semiconductors and insulators: Band gaps and quasiparticle energies, Phys. Rev. B **34**, 5390 (1986).

[39] F. Aryasetiawan and O. Gunnarsson, The GW method, Rep. Prog. Phys. **61**, 237 (1998).

[40] M. Govoni and G. Galli, Large scale GW calculations, J. Chem. Theory Comput. **11**, 2680 (2015).

[41] P. Scherpelz, M. Govoni, I. Hamada, and G. Galli, Implementation and validation of fully relativistic GW calculations: Spin-orbit coupling in molecules, nanocrystals, and solids, J. Chem. Theory Comput. **12**, 3523 (2016).

[42] WEST, http://www.west-code.org (accessed Jan. 26, 2016).

[43] H. F. Wilson, F. Gygi, and G. Galli, Efficient iterative method for calculations of dielectric matrices, Phys. Rev. B **78**, 113303 (2008).

[44] H. F. Wilson, D. Lu, F. Gygi, and G. Galli, Iterative calculations of dielectric eigenvalue spectra, Phys. Rev. B **79**, 245106 (2009).

[45] H.-V. Nguyen, T. A. Pham, D. Rocca, and G. Galli, Improving accuracy and efficiency of calculations of photoemission spectra within the many-body perturbation theory, Phys. Rev. B **85**, 081101(R) (2012).

[46] T. A. Pham, H.-V. Nguyen, D. Rocca, and G. Galli, *GW* calculations using the spectral decomposition of the dielectric matrix: Verification, validation, and comparison of methods, Phys. Rev. B **87**, 155148 (2013).

[47] S. Baroni, S. de Gironcoli, A. D. Corso, and P. Giannozzi, Phonons and related crystal properties from density-functional perturbation theory, Rev. Mod. Phys. **73**, 515 (2001).

[48] See Supplemental Material at http://link.aps.org/supplemental/10.1103/PhysRevMaterials.1.021602 for calculation details, convergence studies, and further results at the PBE level of theory.

[49] J. Wieferink, P. Krüger, and J. Pollmann, *Ab initio* study of atomic hydrogen diffusion on the clean and hydrogen-terminated Si(001) surface, Phys. Rev. B **82**, 075323 (2010).

[50] T. Blomquist and G. Kirczenow, Controlling the charge of a specific surface atom by the addition of a non-site-specific single impurity in a Si nanocrystal, Nano Lett. **6**, 61 (2006).

[51] M. B. Haider, J. L. Pitters, G. A. DiLabio, L. Livadaru, J. Y. Mutus, and R. A. Wolkow, Controlled coupling and occupation of silicon atomic quantum dots, arXiv:0807.0609.

[52] H. Raza, Theoretical study of isolated dangling bonds, dangling bond wires, and dangling bond clusters on a H:Si(001)-2 × 1 surface, Phys. Rev. B **76**, 045308 (2007).

[53] H.-P. Komsa and A. Pasquarello, Finite-Size Supercell Correction for Charged Defects at Surfaces and Interfaces, Phys. Rev. Lett. **110**, 095505 (2013).

[54] Only the lowest two values from Refs. [6,49] are explicitly spin polarized; the calculations that cluster at 0.35–0.42 eV are thus unlikely to be physically accurate.

[55] Y. Li and G. Galli, Electronic and spectroscopic properties of the hydrogen-terminated Si(111) surface from *ab initio* calculations, Phys. Rev. B **82**, 045321 (2010).

[56] M. V. Fischetti, B. Fu, S. Narayanan, and J. Kim, Semiclassical and quantum electronic transport in nanometer-scale structures: Empirical pseudopotential band structure, Monte Carlo simu-

lations and Pauli master equation, in *Nano-Electronic Devices*, edited by D. Vasileska and S. M. Goodnick (Springer, New York, 2011), p. 183.

[57] K. Sagisaka, J. Nara, and D. Bowler, Importance of bulk states for the electronic structure of semiconductor surfaces: Implications for finite slabs, J. Phys.: Condens. Matter **29**, 145502 (2017).

[58] P. M. Lenahan and J. F. Conley, Jr., What can electron paramagnetic resonance tell us about the Si/SiO$_2$ system? J. Vac. Sci. Technol. B **16**, 2134 (1998).

[59] C. Freysoldt, B. Grabowski, T. Hickel, J. Neugebauer, G. Kresse, A. Janotti, and C. G. Van de Walle, First-principles calculations for point defects in solids, Rev. Mod. Phys. **86**, 253 (2014).

[60] Z. Shaterzadeh-Yazdi, L. Livadaru, M. Taucer, J. Mutus, J. Pitters, R. A. Wolkow, and B. C. Sanders, Characterizing the rate and coherence of single-electron tunneling between two dangling bonds on the surface of silicon, Phys. Rev. B **89**, 035315 (2014).

[61] J. Y. Lee, J.-H. Choi, and J.-H. Cho, Antiferromagnetic coupling between two adjacent dangling bonds on Si(001): Total-energy and force calculations, Phys. Rev. B **78**, 081303 (2008).

[62] J. Y. Lee, J.-H. Cho, and Z. Zhang, Quantum size effects in competing charge and spin orderings of dangling bond wires on Si(001), Phys. Rev. B **80**, 155329 (2009).

[63] R. Robles, M. Kepenekian, S. Monturet, C. Joachim, and N. Lorente, Energetics and stability of dangling-bond silicon wires on H passivated Si(100), J. Phys.: Condens. Matter **24**, 445004 (2012).

[64] M. Kepenekian, F. D. Novaes, R. Robles, S. Monturet, H. Kawai, C. Joachim, and N. Lorente, Electron transport through dangling-bond silicon wires on H-passivated Si(100), J. Phys.: Condens. Matter **25**, 025503 (2013).

[65] M. Engelund, N. Papior, P. Brandimarte, T. Frederiksen, A. Garcia-Lekue, and D. Sánchez-Portal, Search for a metallic dangling-bond wire on n-doped H-passivated semiconductor surfaces, J. Phys. Chem. C **120**, 20303 (2016).

[66] M. Zhou, Z. Liu, Z. Wang, Z. Bai, Y. Feng, M. G. Lagally, and F. Liu, Strain-Engineered Surface Transport in Si(001): Complete Isolation of the Surface State via Tensile Strain, Phys. Rev. Lett. **111**, 246801 (2013).

[67] J. Munguía, G. Bremond, J. M. Bluet, J. M. Hartmann, and M. Mermoux, Strain dependence of indirect band gap for strained silicon on insulator wafers, Appl. Phys. Lett. **93**, 102101 (2008).

[68] S. Richard, F. Aniel, G. Fishman, and N. Cavassilas, Energy-band structure in strained silicon: A 20-band k·p and Bir-Pikus Hamiltonian model, J. Appl. Phys. **94**, 1795 (2003).

[69] F. Liu, M. Huang, P. P. Rugheimer, D. E. Savage, and M. G. Lagally, Nanostressors and the Nanomechanical Response of a Thin Silicon Film on an Insulator, Phys. Rev. Lett. **89**, 136101 (2002).

[70] J. Munguía, J.-M. Bluet, O. Marty, G. Bremond, M. Mermoux, and D. Rouchon, Temperature dependence of the indirect bandgap in ultrathin strained silicon on insulator layer, Appl. Phys. Lett. **100**, 102107 (2012).

[71] K. Saeedi, S. Simmons, J. Z. Salvail, P. Dluhy, H. Riemann, N. V. Abrosimov, P. Becker, H.-J. Pohl, J. J. L. Morton, and M. L. W. Thewalt, Room-temperature quantum bit storage exceeding 39 minutes using ionized donors in silicon-28, Science **342**, 830 (2013).

[72] J. J. Pla, K. Y. Tan, J. P. Dehollain, W. H. Lim, J. J. L. Morton, F. A. Zwanenburg, D. N. Jamieson, A. S. Dzurak, and A. Morello, High-fidelity readout and control of a nuclear spin qubit in silicon, Nature (London) **496**, 334 (2013).

[73] J. Salfi, J. A. Mol, R. Rahman, G. Klimeck, M. Y. Simmons, L. C. L. Hollenberg, and S. Rogge, Quantum simulation of the Hubbard model with dopant atoms in silicon, Nat. Commun. **7**, 11342 (2016).

[74] M. H. Mohammady, G. W. Morley, A. Nazir, and T. S. Monteiro, Analysis of quantum coherence in bismuth-doped silicon: A system of strongly coupled spin qubits, Phys. Rev. B **85**, 094404 (2012).

[75] G. Wolfowicz, A. M. Tyryshkin, R. E. George, H. Riemann, N. V. Abrosimov, P. Becker, H.-J. Pohl, M. L. W. Thewalt, S. A. Lyon, and J. J. L. Morton, Atomic clock transitions in silicon-based spin qubits, Nat. Nanotechnol. **8**, 561 (2013).

[76] R. L. Nardo, G. Wolfowicz, S. Simmons, A. M. Tyryshkin, H. Riemann, N. V. Abrosimov, P. Becker, H.-J. Pohl, M. Steger, S. A. Lyon, M. L. W. Thewalt, and J. J. L. Morton, Spin relaxation and donor-acceptor recombination of Se^+ in 28-silicon, Phys. Rev. B **92**, 165201 (2015).

[77] K. J. Morse, R. J. S. Abraham, H. Riemann, N. V. Abrosimov, P. Becker, H.-J. Pohl, M. L. W. Thewalt, and S. Simmons, A photonic platform for donor spin qubits in silicon, arXiv:1606.03488.